Phonon Screening of Excitons in Semiconductors: Halide Perovskites and Beyond

Marina R. Filip,[1,2,3,†] Jonah B. Haber,[2,†] and Jeffrey B. Neaton[2,4,5,*]
[1]Department of Physics, University of Oxford, Oxford OX1 3PJ, United Kingdom
[2]Department of Physics, University of California Berkeley, Berkeley, California 94720, USA
[3]Molecular Foundry, Lawrence Berkeley National Laboratory, Berkeley, California 94720, USA
[4]Materials Science Division, Lawrence Berkeley National Laboratory, Berkeley, California 94720, USA
[5]Kavli Energy NanoSciences Institute at Berkeley, Berkeley, California 94720, USA

(Received 6 March 2020; revised 5 December 2020; accepted 4 June 2021; published 5 August 2021)

The *ab initio* Bethe-Salpeter equation (BSE) approach, an established method for the study of excitons in materials, is typically solved in a limit where only static screening from electrons is captured. Here, we generalize this framework to include dynamical screening from phonons at lowest order in the electron-phonon interaction. We apply this generalized BSE approach to a series of inorganic lead halide perovskites, $CsPbX_3$, with $X = Cl$, Br, and I. We find that inclusion of screening from phonons significantly reduces the computed exciton binding energies of these systems. By deriving a simple expression for phonon screening effects, we reveal general trends for their importance in semiconductors and insulators, based on a hydrogenic exciton model. We demonstrate that the magnitude of the phonon screening correction in isotropic materials can be reliably predicted using four material specific parameters: the reduced effective mass, static and optical dielectric constants, and frequency of the most strongly coupled longitudinal-optical phonon mode. This framework helps to elucidate the importance of phonon screening and its relation to excitonic properties in a broad class of semiconductors.

DOI: 10.1103/PhysRevLett.127.067401

Excitons are central to a wide range of optoelectronic applications, from photovoltaics and photocatalysis, to light emission and lasing [1–4]; they emerge from the many-body interactions between charge carriers, photons, and phonons in optoelectronic materials [5]. In many bulk semiconductors, weakly bound Wannier-Mott excitons can be understood with a hydrogenic model [6,7], in which the attractive Coulomb interaction between a photoexcited electron-hole pair is screened by a dielectric constant ε. In this picture, the exciton binding energy is $\mu/(2\varepsilon^2)$ in atomic units, where μ is the magnitude of the reduced effective mass of the electron-hole pair [6]. Optical measurements under high magnetic fields use this model to extract the exciton binding energy E_B and μ [8,9]. In ionic or multicomponent semiconductors, an "effective dielectric constant" $\varepsilon_{\text{eff}} = \sqrt{2E_B/\mu}$ is frequently reported, usually taking values between the optical ε_∞ and static ε_0 dielectric constants. The use of ε_{eff} approximately accounts for the fact that the electron-hole interaction is screened by both the electrons and phonons [2,10,11]. However, it also obscures the details of specific phonons contributing to ε_{eff}, and it does not explain whether or why electron or phonon screening might be important in a given case. Rigorous *ab initio* calculations would therefore be of great value in this context.

Ab initio many-body perturbation theory calculations within the *GW* approximation [12,13] and the Bethe-Salpeter equation (BSE) [14,15] approach have been successful in quantitatively understanding the quasiparticle band structure and optical excitations of materials ranging from the simplest III–V semiconductors [16] to materials with heavy elements [17] or hybrid organic-inorganic components [18], low dimensionality [19], and intrinsic defects [20]. First principles methods including the effects of lattice vibrations have led to new understanding of the renormalization of the electronic band structure due to electron-phonon interactions [21–23], as well as optical absorption [24,25] and photoluminescence line shapes [26,27].

Recently, several first principles studies of a broad range of materials predicted exciton binding energies that are overestimated with respect to experiment [28–33]. In particular, Ref. [32] recently reported calculated exciton binding energies of hybrid organic-inorganic lead-halide perovskites that overestimate experimental measurements by up to a factor of 3. Reference [32] attributed this overestimation to the coupling of the constituent free electrons and holes to phonons (hereafter referred to as "polaronic effects"). On the other hand, Ref. [33] used an approximate model dielectric function to conclude that phonon screening due to infrared active phonons renormalizes the exciton binding energy by up to 50%, bringing calculated values in much closer agreement with experiment. Since both reports are based on approximate hypotheses and implementations of phonon effects, it is not yet clear how these conclusions may be reconciled, in the

absence of a complete *ab initio* calculation. The problem of electrons and holes interacting in a phonon field has been studied using phenomenological models, assuming parabolic electronic band structure and a phonon spectrum consisting of a single dispersionless phonon [10,11,34–36]. However, rigorous inclusion of polaronic and phonon screening effects within the BSE formalism remains an open challenge.

In this Letter, we extend the standard *ab initio* BSE formalism to include phonon screening effects at lowest order in the electron-phonon interaction. We introduce an additive, $\mathbf{q}$- and ω-dependent contribution to the screened Coulomb interaction W associated with phonons, adopting a general form developed by Hedin and Lundqvist [37] but neglected in contemporary calculations. We apply this framework to a set of all-inorganic lead-halide perovskite crystals in the low-temperature, orthorhombic phase using the *ab initio* Fröhlich electron-phonon vertex introduced in Ref. [38], and we show that phonon screening plays a major, but not exclusive, role in the exciton binding energies of this emergent class of optoelectronic materials. Finally, we develop a simple but general expression for the phonon-screened exciton binding energy for arbitrary isotropic semiconductors in terms of μ, ε_∞, ε_0, and ω_{LO}, providing a means for identifying semiconductors for which phonon screening effects will be significant.

In the standard *ab initio* reciprocal-space *GW*-BSE approach, the BSE can be written, in the Tamm-Dancoff approximation [14,16], as

$$\Delta_{c\mathbf{k}v\mathbf{k}}A^S_{cv\mathbf{k}} + \sum_{c'v'\mathbf{k}'} K_{cv\mathbf{k},c'v'\mathbf{k}'}(\Omega_S)A^S_{c'v'\mathbf{k}'} = \Omega_S A^S_{cv\mathbf{k}}, \quad (1)$$

where $\Delta_{c\mathbf{k}v\mathbf{k}} = E_{c\mathbf{k}} - E_{v\mathbf{k}}$, and where $E_{c\mathbf{k}}$ and $E_{v\mathbf{k}}$ are the quasiparticle energies of the free electron and hole with band indices and wave vectors $c\mathbf{k}$ and $v\mathbf{k}$, respectively, usually calculated within the *GW* approximation [12,13]. Exciton energies and expansion coefficients, in the electron-hole basis, are given by Ω_S and $A^S_{cv\mathbf{k}} = \langle cv\mathbf{k}|S\rangle$, respectively, with S the principal quantum number for the exciton and $|cv\mathbf{k}\rangle$ the product state of an electron-hole pair, where the components of the products here are Kohn-Sham wave functions computed with density functional theory (DFT) [39].

The electron-hole kernel K couples products of the single-particle states and is, at lowest order, written as the sum of two terms, a repulsive exchange term K^x, which is negligible for weakly bound excitons [40], and an attractive direct term K^D, given by, as in Ref. [40],

$$K^D_{cv\mathbf{k},c'v'\mathbf{k}'}(\Omega) = -\left\langle cv\mathbf{k}\left|\frac{i}{2\pi}\int d\omega e^{-i\omega\eta}W(\mathbf{r},\mathbf{r}';\omega)\left[\frac{1}{\Omega-\omega-\Delta_{c'\mathbf{k}'v\mathbf{k}}+i\eta}+\frac{1}{\Omega+\omega-\Delta_{c\mathbf{k}v'\mathbf{k}'}+i\eta}\right]\right|c'v'\mathbf{k}'\right\rangle, \quad (2)$$

where η is a positive infinitesimal quantity, and $W(\mathbf{r},\mathbf{r}';\omega)$ is the time-ordered screened Coulomb interaction, which typically only includes electronic contributions to screening. In general, the BSE must be solved self-consistently, as K^D depends on Ω_S.

As discussed by Hedin and Lundqvist [37], W can rigorously be written as the sum of an electronic W^{el} and ionic (or phonon) W^{ph} part, i.e., $W(\mathbf{r},\mathbf{r}';\omega) = W^{\mathrm{el}}(\mathbf{r},\mathbf{r}';\omega) + W^{\mathrm{ph}}(\mathbf{r},\mathbf{r}';\omega)$. In standard BSE calculations, W^{ph} is ignored, while W^{el} is routinely computed within the random-phase approximation (RPA) [41,42], neglecting the frequency dependence. The W^{ph} term may be written in the form (see Supplemental Material [43])

$$W^{\mathrm{ph}}(\mathbf{r},\mathbf{r}';\omega) = \sum_{\mathbf{q}\nu} D_{\mathbf{q}\nu}(\omega)g_{\mathbf{q}\nu}(\mathbf{r})g^*_{\mathbf{q}\nu}(\mathbf{r}'), \quad (3)$$

where $D_{\mathbf{q}\nu}(\omega)$ is the phonon propagator and $g_{\mathbf{q}\nu}(\mathbf{r})$ is the electron-phonon vertex, encoding the probability amplitude for an electron at $\mathbf{r}$ to scatter off a phonon with crystal momentum $\mathbf{q}$ and branch index ν [37] (also see Supplemental Material [43]).

Incorporating W^{ph} into the BSE kernel, we obtain the phonon contribution to the real part of the direct electron-hole kernel matrix elements as follows (written here in the exciton basis; see Supplemental Material for details [43]):

$$\mathrm{Re}[K^{\mathrm{ph}}_{SS'}(\Omega)] = -\sum_{\substack{cv\mathbf{k}\\ c'v'\mathbf{k}'\nu}} A^{S*}_{cv\mathbf{k}}g_{cc'\nu}(\mathbf{k}',\mathbf{q})g^*_{vv'\nu}(\mathbf{k}',\mathbf{q})A^{S'}_{c'v'\mathbf{k}'} \times\left[\frac{1}{\Omega-\Delta_{c'\mathbf{k}'v\mathbf{k}}-\omega_{\mathbf{q}\nu}}+\frac{1}{\Omega-\Delta_{c\mathbf{k}v'\mathbf{k}'}-\omega_{\mathbf{q}\nu}}\right], \quad (4)$$

where $g_{nm\nu}(\mathbf{k}',\mathbf{q}) = \langle m\mathbf{k}'+\mathbf{q}|g_{\mathbf{q}\nu}|n\mathbf{k}'\rangle$, with $\mathbf{q} = \mathbf{k}-\mathbf{k}'$. From Brillouin-Wigner perturbation theory, it follows that the change in the exciton energy $\Delta\Omega_S$, due to phonon screening, is related to K^{ph} through $\Delta\Omega_S = \mathrm{Re}[K^{\mathrm{ph}}_{SS}(\Omega_S+\Delta\Omega_S)]$, in the limit where off-diagonal components of K^{ph} can be neglected.

We pause to note that W^{ph} should, in principle, be included in both the BSE kernel and *GW* self-energy. The contribution to the latter, i.e., iGW^{ph}, is equivalent to the Fan-Migdal electron-phonon self-energy [21] and leads to polaronic mass enhancement and energy renormalization (e.g., [65]) effects that would naively tend to increase the exciton binding energy over the bare or phonon-screened values. However as discussed in Ref. [10], interference between electron and hole polaron clouds upon overlap (hereafter referred to as "interference effects") can counter mass enhancement effects, reducing the overall binding energy. A full *ab initio* study of bound electron-hole

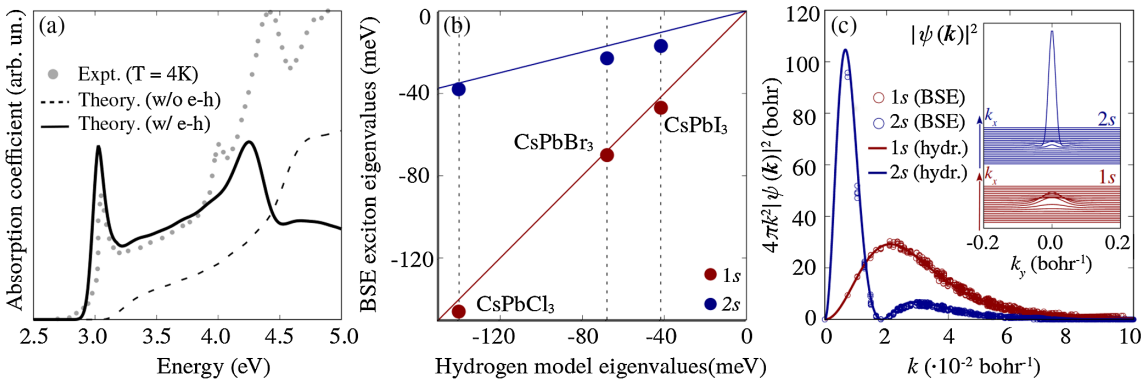

FIG. 1. (a) Optical absorption spectrum calculated within GW/BSE (continuous line), RPA (dotted line), and from experiment (Expt; gray dots) for $CsPbCl_3$; experimental data is extracted from Ref. [72]. Calculated spectra are blueshifted by 0.3 eV to match the experimental onset from Ref. [72]. See Supplemental Material for similar spectra for $CsPbBr_3$ and $CsPbI_3$ [43]. (b) Exciton binding energies predicted from GW/BSE (filled circles) and the hydrogen model (lines). (c) Exciton radial probability density (main) and probability of localization (inset) in reciprocal space, calculated from GW/BSE and the hydrogen model (hydr.) for $1s$ (dark red) and $2s$ (dark blue) states.

polarons, including the competition between mass enhancement and interference effects, as described by higher-order or self-consistent terms in the BSE kernel, requires a separate study and is beyond the scope of this work; thus, we restrict our focus here to quantifying and understanding the phonon screening contribution to the exciton binding energy, building on prior work [31,33] and the standard GW approximation in all cases.

We now apply Eqs. (1) and (2), as implemented in the BerkeleyGW code [66], to $CsPbX_3$ lead-halide perovskites, with $X = \mathrm{Cl}$, Br, I. In Table I we compare calculated G_0W_0 band gaps and reduced effective masses to experiment. The computed gaps consistently underestimate experiment by up to 0.5 eV (see Table S2 of the Supplemental Material [43]), a shortcoming of one-shot G_0W_0 approximation previously identified in a number of computational studies [18,67–69]. Furthermore, the reduced effective masses of $CsPbI_3$ and $CsPbBr_3$ agree well with recent magneto-optical measurements at high magnetic fields, while for $CsPbCl_3$ the reduced mass is slightly underestimated with respect to experiment [8,70]. In the same table, we also report exciton binding energies calculated within the standard BSE approach, including only electronic screening when constructing the electron-hole kernel. In agreement with previous calculations [32,33], we find that exciton binding energies neglecting phonon screening overestimate experiment by up to a factor of 3. Despite these discrepancies, after blueshifting the calculated optical absorption spectrum to align with experiment, we find the line shape to be in good agreement with measurements at low temperature [Fig. 1(a) for $CsPbCl_3$ and Fig. S2 for $CsPbBr_3$ and $CsPbI_3$].

We further observe that low-lying optical excitations are well described using a Mott-Wannier hydrogen model. In Fig. 1(b), we compare the BSE solutions for the $1s$ and $2s$ excitonic states with those predicted by the hydrogen model, with μ calculated from G_0W_0 band structure and with ε_∞ calculated within the RPA [41,42]. We find a maximum difference between the hydrogenic model and the standard BSE calculations of 6 meV for both $1s$ and $2s$ excitonic energies across all three halide perovskites. Furthermore, in Fig. 1(c), we find that the excitonic wave functions calculated with BSE are accurately described by the hydrogenic model.

We now investigate how including phonon screening contributions shifts the energy of the lowest bound exciton by explicitly computing K^{ph}. We make two approximations to Eq. (4): we use the analytic hydrogenic expressions for

TABLE I. Calculated longitudinal-optical (LO) phonon frequencies (ω_{LO}), bare exciton binding energies (E_B), phonon screening corrections (ΔE_B), reduced effective masses (μ), static (ε_0 from density functional perturbation theory; DFPT [71]) and optical dielectric constants (ε_∞ from DFPT and G_0W_0), and corresponding experimental data from the indicated references.

	ω_{LO} (meV)	$\omega_{\mathrm{LO}}^{\mathrm{exp}}$ (meV)	E_B (meV)	ΔE_B (meV)	E_B^{exp} (meV)	μ (m_e)	μ^{exp} (m_e)	ε_∞	$\varepsilon_\infty^{\mathrm{exp}}$	ε_0	$\varepsilon_0^{\mathrm{exp}}$
$CsPbCl_3$	26	25.3/28.0 [73]; 27.5 [74]	146	−17	72±3 [75]; 64±1.5 [76]	0.142	0.202±0.01 [76]	3.7	3.7 [73]	17.5	15.7 [73]
$CsPbBr_3$	18	17.9/20.4 [77]	70	−12	33±1 [78]; 38±3 [75]	0.102	0.126±0.02 [78]	4.5	⋯	18.6	⋯
$CsPbI_3$	14	14.2 [79]	47	−8	15±1 [78]	0.093	0.114±0.01 [78]	5.5	⋯	22.5	⋯

the exciton coefficients $A^S_{cv\mathbf{k}}$, and we approximate the electron-phonon matrix elements using a multimode, *ab initio* Fröhlich vertex, introduced in Ref. [38],

$$g_{\mathbf{q}\nu} = i\frac{4\pi}{V}\sum_{\kappa}\left(\frac{1}{2NM_\kappa\omega_{\mathbf{q}\nu}}\right)^{1/2}\frac{\mathbf{q}\cdot\mathbf{Z}_\kappa\cdot\mathbf{e}_{\kappa\nu}(\mathbf{q})}{\mathbf{q}\cdot\boldsymbol{\varepsilon}_\infty\cdot\mathbf{q}}, \quad (5)$$

where V is the unit cell volume, M_κ are the atomic masses, $\mathbf{Z}_\kappa$ is the Born effective charge tensor, and $\mathbf{e}_{\kappa\nu}(\mathbf{q})$ are the eigenvectors corresponding to the phonon modes $\omega_{\mathbf{q}\nu}$ for each atom indexed by κ. With the above simplifications, Eq. (4) becomes

$$\Delta\Omega_S = -\frac{8a_0^3}{\pi^2}\sum_{\mathbf{k}\mathbf{q}\nu}\frac{|g_{\mathbf{q}\nu}|^2}{[1+a_0|\mathbf{k}|^2]^2[1+a_0^2|\mathbf{k}+\mathbf{q}|^2]^2}\left[\frac{1}{\Omega_S-\Delta_{c\mathbf{k}v'\mathbf{k}+\mathbf{q}}-\omega_{\mathbf{q}\nu}}+\frac{1}{\Omega_S-\Delta_{c'\mathbf{k}+\mathbf{q}v\mathbf{k}}-\omega_{\mathbf{q}\nu}}\right], \quad (6)$$

where a_0 is the exciton Bohr radius. In principle, Ω_S appearing in the energy denominator above should be replaced with $\Omega_S+\Delta\Omega_S$ and the equation should be solved self-consistently. In practice, for $CsPbX_3$ we find the above expression differs by less than 1 meV from the self-consistent solution justifying a "one-shot" approach. Finally, by definition, the change in the exciton binding energy is $\Delta E_B = -\Delta\Omega_S$.

The standard BSE exciton binding energies and phonon screening corrections are summarized in Table I for all three $CsPbX_3$ perovskites. We find that phonon screening contributes to the reduction of the exciton binding energy between 12% and 17% for the $CsPbX_3$ series, improving the agreement with measurements reported in Refs. [75,76,78]. However, for $CsPbI_3$, our calculated relative phonon screening correction of 17% is less than half of the 50% correction predicted in Ref. [33]; as we show in the following, this discrepancy can be attributed to electronic band dispersion contributions, accounted for here but neglected in prior work.

To further investigate the contribution of phonon screening to the exciton binding energy, we perform a spectral decomposition on the phonon kernel (see Fig. S4 of the Supplemental Material [43]). For all three halide perovskites (see Supplemental Material [43]), we find that the contribution of the highest lying IR active phonons accounts for more than 90% of the expectation value of K^{ph}, with the remaining contribution due to the lower energy LO modes. Furthermore, as shown in Fig. S4, the phonon kernel drops sharply outside of the $\mathbf{q}\to 0$ range, a trend attributed to the strong localization of the exciton wave function around the center of the Brillouin zone and the fast decay of the long-range electron-phonon vertex in reciprocal space.

Given the flat profile of the optical phonon band shown in Fig. S4, we can further simplify the phonon kernel by replacing the phonon frequencies with ω_{LO} and approximating the electron-phonon vertex in Eq. (6) using the Fröhlich model [80], $|g^F_{\mathbf{q}}|^2 = 4\pi\omega_{\mathrm{LO}}/(2NV)(\varepsilon_\infty^{-1}-\varepsilon_0^{-1})/q^2$, where N is the total number of unit cells in the crystal. This approximation yields a change in the phonon screening correction of $\sim$1% with respect to the *ab initio* result, indicating that the single dispersionless phonon model is a suitable approximation for the phonon kernel in these systems. Assuming isotropic and parabolic electronic band dispersion, Eq. (6) can be solved analytically (see the Supplemental Material for details [43]), obtaining

$$\Delta E_B = -2\omega_{\mathrm{LO}}\left(1-\frac{\epsilon_\infty}{\varepsilon_0}\right)\frac{\sqrt{1+\omega_{\mathrm{LO}}/E_B}+3}{(1+\sqrt{1+\omega_{\mathrm{LO}}/E_B})^3}. \quad (7)$$

For isotropic semiconductors, Eq. (7) yields very close agreement with the numerical evaluation of Eq. (6) (see Table S4 of the Supplemental Material [43]).

Since the exciton wave function is highly localized at the center of the Brillouin zone (see Fig. S4 of the Supplemental Material [43]), it is tempting to assume that the dispersion of the electronic band structure may also be neglected. This approximation leads to an even simpler expression for the change in the exciton binding energy $\Delta E_B = -2E_B[\omega_{\mathrm{LO}}/(\omega_{\mathrm{LO}}+E_B)](1-\epsilon_\infty/\epsilon_0)$ (see Supplemental Material [43]); however, we find that it overestimates the magnitude of the phonon screening contribution by up to 50% with respect to the *ab initio* result for these systems.

To examine phonon screening trends across a wide range of semiconductors and insulators, we plot the phonon kernel relative to the bare exciton binding energy E_B, $|\Delta E_B|/E_B$, as a function of E_B/ω_{LO}, and $\varepsilon_0/\varepsilon_\infty$, in Fig. 2, following Eq. (7). We overlay our calculations for the $CsPbX_3$ series, as well as some other isotropic semiconductors and insulators such as CdS, GaN, AlN, and MgO (see Supplemental Material for computational details [43]). In all cases considered, the inclusion of phonon screening effects reduces the exciton binding energy significantly, bringing calculated values in closer agreement with experiment.

Particularly for halide perovskites, our calculations reconcile prior reports and clearly establish the importance of phonon screening effects for excitons in halide perovskites, in agreement with Ref. [33]. However, corrections due to phonon screening do not fully account for the discrepancy between calculated and measured exciton binding energies. Considering the systematic overestimation of exciton binding energies for all systems beyond halide perovskites, we expect that the net contribution of

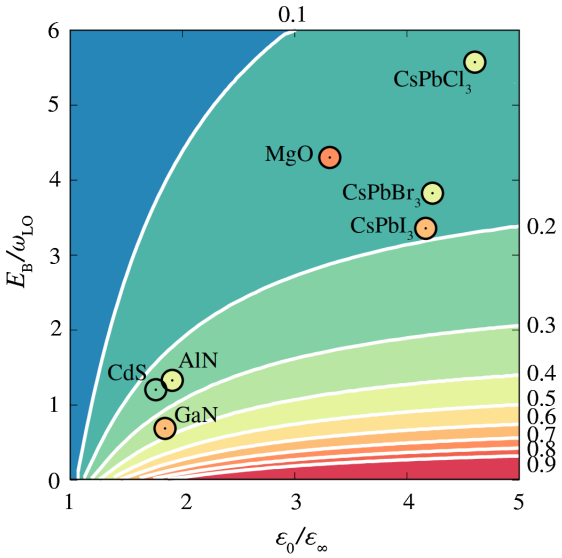

FIG. 2. Color map of $\Delta E_B/E_B$, calculated using Eq. (7), as a function of $\varepsilon_0/\varepsilon_\infty$ and E_B/ω_{LO}. The isoline values are marked at the upper and rightmost edge of the plot. The color of each circle corresponds to the ratio $(E_B - E_B^{exp})/E_B$, as read on the color map. Calculated and experimental exciton binding energies are summarized in Table S4 [43].

polaronic mass enhancement [65] and interference effects [10] will further reduce the exciton binding energies and improve the agreement with experiment, as proposed by Refs. [10,11] for MgO and several other semiconductors. However, G_0W_0-BSE calculations of halide perovskites are known to exhibit a strong dependence on the DFT mean-field starting point [68], and the electron-phonon matrix elements, computed from the standard Kohn-Sham eigensystem, may underestimate couplings obtained from higher-level theory [81–83]. Therefore, a detailed benchmarking of these effects is required, in addition to simply including polaronic effects. While we reserve this detailed analysis for future studies, we emphasize that the relative phonon screening correction derived in this Letter is robust, and the formalism introduced here is independent of the choice of computational setup.

As a general trend, Fig. 2 highlights that the magnitude of the phonon screening correction increases as the ratio E_B/ω_{LO} decreases and in systems with a large static dielectric constant. Further, all parameters appearing in Eq. (7) and depicted in Fig. 2 can be readily computed or measured experimentally so that this simplified picture can be used in both theoretical and experimental contexts to directly assess the expected phonon screening correction to the bare exciton binding energy and identify systems for which phonon screening is expected to be significant.

In summary, we generalized the *ab initio* Bethe-Salpeter equation approach to include both electronic and phonon contributions to the screened Coulomb interaction W and studied phonon screening effects on the electron-hole interactions in halide perovskites and other important semiconductors. We showed that *ab initio* BSE calculations including phonon screening can reduce the exciton binding energy of lead-halide perovskites significantly as compared to electronic screening alone, reconciling two previous contradictory hypotheses on the importance of phonon screening in metal-halide perovskites. We rationalized our results by generalizing the Wannier-Mott model for excitons in a phonon-screened environment. Within this model, we showed that phonon screening is important for other semiconductors and can be traced back to four material-specific parameters: μ, ω_{LO}, ε_∞, and ε_0. We derived a simple expression providing intuition for the importance of lattice vibrations on the excitonic properties of materials and outlined a general, simple, and quantitative approach to estimate the exciton binding energy correction using physical quantities that can be readily calculated theoretically or measured experimentally. By introducing a general framework to quantitatively account for phonon screening in *ab initio* BSE calculations, our Letter clarifies the importance of phonon screening corrections and provides a necessary foundation for future treatment of polarons and higher-order processes beyond two particle excitations for these and other complex materials.

The authors acknowledge A. Alvertis (Berkeley Lab.), D. Qiu (Yale U.), F. da Jornada (Stanford U.), Z. Li (UC Berkeley), and H. Paudial and R. Margine (SUNY Binghamton) for useful discussions. This work was supported by the Theory of Materials Program at the Lawrence Berkeley National Laboratory through the Office of Basic Energy Sciences, U.S. Department of Energy under Contract No. DE-AC02-05CH11231. M. R. F. acknowledges support from the Engineering and Physical Sciences Research Council (EPSRC), Grant No. EP/V010840/1. The authors acknowledge computational resources provided by the National Energy Research Scientific Computing Center (NERSC) and Molecular Foundry, also supported by the Office of Science, Office of Basic Energy Sciences, of the U.S. DOE under Award No. DE-AC02-5CH11231. Additional computational resources were provided by the Extreme Science and Engineering Discovery Environment (XSEDE) supercomputer Stampede2 at the Texas Advanced Computing Center (TACC) through the allocation TG-DMR190070.

*jbneaton@lbl.gov
†M. R. F. and J. B. H. contributed equally to this work.

[1] K. Takanabe, ACS Catal. **7**, 8006 (2017).
[2] L. M. Herz, J. Phys. Chem. Lett. **9**, 6853 (2018).
[3] X. Ai, E. W. Evans, S. Dong, A. J. Gillett, H. Guo, Y. Chen, T. J. H. Hele, R. H. Friend, and F. Li, Nature (London) **563**, 536 (2018).
[4] N. S. Ginsberg and W. A. Tisdale, Annu. Rev. Phys. Chem. **71**, 1 (2020).

[5] R. S. Knox, *Theory of Excitons* (Academic, New York, 1963).
[6] G. H. Wannier, Phys. Rev. **52**, 191 (1937).
[7] R. J. Elliot, Phys. Rev. **108**, 1384 (1957).
[8] A. Miyata, A. Mitioglu, P. Plochocka, O. Portugall, J. T.-W. Wang, S. D. Stranks, and H. J. Snaith, Nat. Phys. **11**, 582 (2015).
[9] P. C. Makado and N. C. McGill, J. Phys. Chem. C **19**, 873 (1986).
[10] S. D. Mahanti and C. M. Varma, Phys. Rev. Lett. **25**, 1115 (1970).
[11] S. D. Mahanti and C. M. Varma, Phys. Rev. B **6**, 2209 (1972).
[12] L. Hedin, Phys. Rev. **139**, A796 (1965).
[13] M. S. Hybertsen and S. G. Louie, Phys. Rev. B **34**, 5390 (1986).
[14] M. Rohlfing and S. G. Louie, Phys. Rev. Lett. **81**, 2312 (1998).
[15] S. Albrecht, L. Reining, R. Del Sole, and G. Onida, Phys. Rev. Lett. **80**, 4510 (1998).
[16] M. Rohlfing and S. G. Louie, Phys. Rev. B **62**, 4927 (2000).
[17] B. Malone and M. L. Cohen, J. Phys. Condens. Matter. **25**, 105503 (2013).
[18] M. R. Filip and F. Giustino, Phys. Rev. B **90**, 245145 (2014).
[19] D. Y. Qiu, F. H. da Jornada, and S. G. Louie, Phys. Rev. Lett. **111**, 216805 (2013).
[20] S. Refaely-Abramson, D. Y. Qiu, S. G. Louie, and J. B. Neaton, Phys. Rev. Lett. **121**, 167402 (2018).
[21] F. Giustino, Rev. Mod. Phys. **89**, 015003 (2017).
[22] F. Giustino, S. G. Louie, and M. L. Cohen, Phys. Rev. Lett. **105**, 265501 (2010).
[23] G. Antonius, S. Poncé, P. Boulanger, M. Cote, and X. Gonze, Phys. Rev. Lett. **112**, 215501 (2014).
[24] J. Noffsinger, E. Kioupakis, C. G. Van de Walle, S. G. Louie, and M. L. Cohen, Phys. Rev. Lett. **108**, 167402 (2012).
[25] M. Zacharias, C. E. Patrick, and F. Giustino, Phys. Rev. Lett. **115**, 177401 (2015).
[26] A. Marini, Phys. Rev. Lett. **101**, 106405 (2008).
[27] G. Antonius and S. Louie, arXiv:1705.04245.
[28] F. Bechstedt, K. Seino, P. H. Hahn, and W. G. Schmidt, Phys. Rev. B **72**, 245114 (2005).
[29] F. Fuchs, C. Rödl, A. Schleife, and F. Bechstedt, Phys. Rev. B **78**, 085103 (2008).
[30] A. Schleife, M. D. Neumann, N. Esser, Z. Galazka, A. Gottwald, J. Nixdorf, R. Goldhahn, and M. Feneberg, New J. Phys. **20**, 053016 (2018).
[31] F. Bechstedt and J. Forthmüller, Appl. Phys. Lett. **114**, 122101 (2019).
[32] M. Bokdam, T. Sander, A. Stroppa, S. Picozzi, D. D. Sarma, C. Franchini, and G. Kresse, Sci. Rep. **6**, 1 (2016).
[33] P. Umari, E. Mosconi, and F. De Angelis, J. Phys. Chem. Lett. **9**, 620 (2018).
[34] J. Pollmann and H. Büttner, Phys. Rev. B **16**, 4480 (1977).
[35] E. O. Kane, Phys. Rev. B **18**, 6849 (1978).
[36] M. Matsuura and H. Büttner, Phys. Rev. B **21**, 679 (1980).
[37] L. Hedin and S. Lundqvist, Solid State Phys. **23**, 1 (1970).
[38] C. Verdi and F. Giustino, Phys. Rev. Lett. **115**, 176401 (2015).
[39] P. Hohenberg and W. Kohn, Phys. Rev. **136**, B864 (1964).
[40] G. Strinati, Riv. Nuovo Cimento **11**, 1 (1988).
[41] S. L. Adler, Phys. Rev. **126**, 413 (1962).
[42] N. Wiser, Phys. Rev. **129**, 62 (1963).
[43] See Supplemental Material at http://link.aps.org/supplemental/10.1103/PhysRevLett.127.067401 for computational and methodological details, and additional figures. Supplemental Material includes additional Refs [44–64].
[44] M. R. Linaburg, E. T. McClure, J. D. Majher, and P. M. Woodward, Chem. Mater. **29**, 3507 (2017).
[45] R. J. Sutton, M. R. Filip, A. A. Haghighirad, N. Sakai, W. Bernard, F. Giustino, and H. J. Snaith, ACS Energy Lett. **3**, 1787 (2018).
[46] J. P. Perdew and A. Zunger, Phys. Rev. B **23**, 5048 (1981).
[47] P. Gianozzi *et al.*, J. Phys. Condens. Matter. **21**, 395502 (2009).
[48] D. R. Hamann, Phys. Rev. B **88**, 085117 (2013).
[49] M. J. van Setten, M. Giantomassi, E. Bousquet, M. J. Verstraete, D. R. Hammann, X. Gonze, and G.-M. Rignanese, Comput. Phys. Commun. **226**, 39 (2018).
[50] R. W. Godby and R. J. Needs, Phys. Rev. Lett. **62**, 1169 (1989).
[51] J. Deslippe, G. Samsonidze, M. Jain, M. L. Cohen, and S. G. Louie, Phys. Rev. B **87**, 165124 (2013).
[52] M. R. Filip, C. Verdi, and F. Giustino, J. Phys. Chem. C **119**, 25209 (2015).
[53] C. L. Davies, M. R. Filip, J. B. Patel, T. W. Crothers, C. Verdi, A. D. Wright, R. L. Milot, F. Giustino, M. B. Johnston, and L. M. Herz, Nat. Commun. **9**, 293 (2018).
[54] P. Scherpelz, M. Govoni, I. Hamada, and G. Galli, J. Chem. Theory Comput. **12**, 3523 (2016).
[55] C. K. N. Moller, Nature (London) **182**, 1436 (1958).
[56] M. A. Pérez-Osorio, R. L. Milot, M. R. Filip, J. B. Patel, L. M. Herz, M. B. Johnston, and F. Giustino, J. Phys. Chem. C **119**, 25703 (2015).
[57] J. F. Muth, J. H. Lee, I. K. Shmagin, and R. M. Kolbas, Appl Phys. Lett. **71**, 2572 (1997).
[58] R. A. R. Leute, M. Feneberg, K. Sauer, R. Thonke, S. B. Thapa, F. Scholz, Y. Taniyasu, and M. Kasu, Appl. Phys. Lett. **95**, 031903 (2009).
[59] J. Li, K. B. Nam, M. L. Nakarmi, J. Y. Lin, H. X. Jiang, P. Carrier, and S.-H. Wei, Appl. Phys. Lett. **83**, 5163 (2003).
[60] W. C. Walker, D. M. Roessler, and E. Loh, Phys. Rev. Lett. **20**, 847 (1968).
[61] R. C. Whited, C. J. Flaten, and W. C. Walker, Solid State Commun. **13**, 1903 (1973).
[62] O. Madelung, *Semiconductors Data Handbook* (Springer-Verlag, Berlin, Heidelberg, 2004).
[63] M. A. Jakobson, V. D. Kagan, R. P. Seisyan, and E. V. Goncharova, J. Cryst. Growth **138**, 225 (1994).
[64] J. Voigt, F. Spielberg, and M. Seononer, Phys. Status Solidi **91**, 189 (1979).
[65] M. Schlipf, S. Ponce, and F. Giustino, Phys. Rev. Lett. **121**, 086402 (2018).
[66] J. Deslippe, G. Samsonidze, D. A. Strubbe, M. Jain, M. L. Cohen, and S. G. Louie, Comput. Phys. Commun. **183**, 1269 (2012).
[67] F. Brivio, K. T. Butler, A. Walsh, and M. van Schilfgaarde, Phys. Rev. B **89**, 155204 (2014).
[68] L. Leppert, T. Rangel, and J. B. Neaton, Phys. Rev. Mater. **3**, 103803 (2019).
[69] J. Wiktor, U. Rothlisberger, and A. Pasquarello, J. Phys. Chem. Lett. **8**, 5507 (2017).

[70] M. Baranowski and P. Plochocka, Adv. Energy Mater. **10**, 1903659 (2020).
[71] S. Baroni, S. de Gironcoli, A. Dal Corso, and P. Gianozzi, Rev. Mod. Phys. **73**, 515 (2001).
[72] K. Heindrich, H. Künzel, and J. Treusch, Solid State Commun. **25**, 887 (1978).
[73] C. Carabatos-Nedelec, M. Ousaïd, and K. Nitsch, J. Raman Spectrosc. **34**, 388 (2003).
[74] K. Wakamura and Y. Noda, J. Phys. Chem. Solids **62**, 2027 (2001).
[75] Q. Zhang, R. Su, X. Liu, T. C. Sum, and Q. Xiong, Adv. Funct. Mater. **26**, 6238 (2016).
[76] M. Baranowski, P. Plochocka, R. Su, L. Legrand, T. Barisien, F. Bernardot, Q. Xiong, C. Testelin, and M. Chamarro, Photonics Res. **8**, A50 (2020).
[77] C. M. Iaru, J. J. Geuchies, P. M. Koenraad, D. Vanmaekelbergh, and A. Y. Silov, ACS Nano **11**, 11024 (2017).
[78] Z. Yang, A. Surrente, K. Galkowski, A. Miyata, O. Portugall, R. J. Sutton, A. A. Haghighirad, H. J. Snaith, D. K. Maude, P. Plochocka, and R. J. Nicholas, ACS Energy Lett. **2**, 1621 (2017).
[79] F. Zhao, J. Li, X. Gao, X. Qiu, X. Lin, T. He, and R. Chen, J. Phys. Chem. C **123**, 9538 (2019).
[80] H. Fröhlich, J. Adv. Phys. **3**, 325 (1954).
[81] J. L. Janssen, M. Cote, S. G. Louie, and M. L. Cohen, Phys. Rev. B **81**, 073106 (2010).
[82] G. Antonius, S. Poncé, P. Boulanger, M. Côté, and X. Gonze, Phys. Rev. Lett. **112**, 215501 (2014).
[83] Z. Li, G. Antonius, M. Wu, F. H. da Jornada, and S. G. Louie, Phys. Rev. Lett. **122**, 186402 (2019).